Multiple photon antibunching-to-bunching transitions in the dissipative anisotropic quantum Rabi model

Tian Ye^{1,2}, Chen Wang³,* and Qing-Hu Chen^{1,2,†}

¹ Zhejiang Province Key Laboratory of Quantum Technology and Device,

Department of Physics, Zhejiang University, Hangzhou 310027, China

² Collaborative Innovation Center of Advanced Microstructures, Nanjing University, Nanjing 210093, China

³ Department of Physics, Zhejiang Normal University, Jinhua 321004, Zhejiang, China

(Dated: January 7, 2022)

We investigate the two-photon correlation function in the dissipative anisotropic quantum Rabi model in the framework of quantum dressed master equation. Multiple antibunching-to-bunching transitions are generally exhibited at the deep strong qubit-photon coupling. The emerged additional photon antibunching feature is however lacking in the dissipative isotropic quantum Rabi model. Importantly, the observed two-photon statistics can be well described analytically within a few lowest eigenstates at low temperatures. It is revealed that the additional photon antibunching effect is mainly originated from the selection rule of the two-photon correlation measurement induced eigenstate transitions and the enlarged energy gap of the first two eigenstates after the level crossings. Moreover, we unravel the implication of the photon bunching behavior with the first-order quantum phase transition. We hope these results may fertilize the analysis of the nonclassical photon radiation in the anisotropic qubit-photon hybrid systems.

PACS numbers: 42.50.Ct, 42.50.Ar, 03.65.Yz

I. INTRODUCTION

Deep understanding and smart manipulation of quantum light-matter interaction becomes a challenging interdisciplinary frontier, which is scientifically important and practically demanding in the quantum community [1, 2]. One representative paradigm to theoretically describe quantum light-matter interaction is the qubit-photon hybrid quantum system [3, 4], i.e., a multitasking platform for complementary functionalities with different physical components (e.g., qubit and optical resonator), which has been extensively investigated in diverse fields, ranging from quantum optics [5, 6], quantum information [7, 8], quantum phase transition (QPT) [9-13], to quantum transport [14–17]. The experimental realizations of the ultrastrong qubit-photon coupling [18–20] stimulate the researchers to explore uncharted regimes of hybrid quantum systems.

The quantum Rabi model (QRM) [21–25] is widely considered as the generic model to characterize qubit-photon hybrid systems, which is composed of one qubit interacting with a single-mode radiation field. Traditionally, the qubit-photon coupling in the quantum electrodynamics platforms, e.g., natural atoms in resonant cavity, is rather weak [26], which reduces the QRM to the Jaynes-Cummings model [27] (JCM) by performing the rotating-wave-approximation. However, along with the dramatic advance of solid-state quantum platforms, such as circuit quantum electrodynam-

ics system [20, 28–30], the intriguing ultrastrong interaction has attracted tremendous attention [5–7], where the qubit-photon coupling strength is comparable to the individual components energies. This directly invalidates the rotating-wave-approximation. Consequently, the counter-rotating-wave (CRW) terms produce a series of exciting physical phenomena, e.g., parity symmetry restricted photon-wave-packet propagation [31], vacuum Rabi splitting [32], one photon simultaneously exciting two atoms [33], and multiphoton sidebands transition [34].

Aimed to bridge the gap between the JCM and QRM, the anisotropic quantum Rabi model (AQRM) was proposed [35, 36], where the strengths of the rotating-wave (RW) and CRW terms are relaxed to be independent. In the weak CRW terms limit, the AQRM is shifted to the JCM, whereas the AQRM becomes QRM with identical coupling strengths for both RW and CRW terms. The AQRM nowadays can be realized by various quantum platforms, such as inductively coupled circuit quantum electrodynamics systems [37–39], two-dimensional electron gas with spin-orbit coupling [40], and a twolevel qubit exchanging spin with one anisotropic ferromagnet [41]. By exploring the energy spectrum of the AQRM, the 1st-order QPT is observed when the CRW terms are weaker than RW terms [36], which is, in sharp contrast, absent in the QRM. Very recently, Chen et al. reported that the AQRM undergoes infinitely 1st-order QPT by continuously increasing the qubit-photon coupling strength [11].

In reality, the qubit-photon hybrid quantum system inevitably interacts with the environment [42]. The system-bath interaction induced quantum dissipation will dramatically renew both transient and steady-state behaviors of hybrid quantum systems, e.g., JCM and

 $^{{\}rm *Electronic~address:~wang chenyifang@gmail.com}$

[†]Electronic address: qhchen@zju.edu.cn

QRM, which results in dissipative QPT [43–47]. While from the photon statistics perspective, quantum dissipation enables the reasonable measurements of nonclassical photon statistics [48]. Two-photon correlation function is widely considered as the main observable to characterize the nonclassicality of output photons, which is originally introduced by Glauber to investigate the optical coherence of quantum theory [49]. However, due to the realizations of ultrastrong qubit-photon coupling [5, 6]. the system-bath interaction should be properly treated in the eigenstate framework of the whole hybrid quantum systems [50–53]. In particular, Ridolfo et al. recently proposed a modified definition of the two-photon correlation function to characterize steady-state photon statistics in the dissipative QRM [54–57], based the quantum dressed master equation (DME)[50]. Interestingly, the pronounced antibunching feature is exhibited, which demonstrates the photon blockade [55]. Moreover, the photon blockade has also been unraveled in driven dissipative JCM [46, 47, 58, 59]. Therefore, we naturally raise the questions: (1) What is the new picture of the photon statistics, e.g., photon bunching and photon antibunching, in the dissipative AQRM? (2) Could the nonclassicality of photons of the AQRM coupled to the thermal baths at low temperature keep the trace of the 1st-order QPT in the closed AQRM?

In this work, we apply the modified expression of the two-photon correlation function in Ref. [54] to investigate nonclassical photon behaviors in the dissipative AQRM, where the dissipative dynamics is characterized by the DME. We will focus on the effect of the anisotropic qubitphoton interaction on two-photon statistics in the deep strong coupling regime. We also reveal the implication of the multiple level crossings of the first two eigenstates with the observed bunching and antibunching behavior in the analytical sense. The paper is organized as follows: In Sec. II, we give a brief introduction to the anisotropic quantum Rabi model, the dressed master equation and two photon correlation function. In Sec. III, we numerically show the diagram of the steady-state two photon correlation function of the output field, and analyze the emerging antibunching region and sharp bunching region. We give a conclusion in the last section. The bunching feature of photons in the dissipative quantum Rabi-Stark model is discussed in the Appendix.

II. MODEL AND METHOD

A. Anisotropic quantum Rabi model

The Hamiltonian of AQRM is described as [11, 36]

$$H_{\text{AQRM}} = \omega_0 a^{\dagger} a + \frac{\Delta}{2} \sigma_z + g \left[(a\sigma_+ + a^{\dagger} \sigma_-) + r (a\sigma_- + a^{\dagger} \sigma_+) \right], (1)$$

where a^{\dagger} (a) creates (annihilates) a photon in the cavity with the frequency ω_0 , Δ is the energy splitting of

qubit, $\sigma_{\pm} = \frac{1}{2}(\sigma_x \pm i\sigma_y)$ excites (relaxes) the qubit from the state $|0(1)\rangle$ to $|1(0)\rangle$, with $\sigma_{\alpha=x,y,z}$ the Pauli operators and $|0(1)\rangle$ the qubit ground (excited) state, g is the qubit-photon coupling strength, and r is the anisotropic parameter.

When r=1, the AQRM is reduced to QRM. Furthermore, as the qubit-cavity coupling becomes weak, the CRW terms $(a\sigma_- + a^\dagger \sigma_+)$ become negligible. Under the rotating-wave-approximation, the QRM is reduced to the JCM [27], which is identical with the r=0 limit. Here, the AQRM ties the QRM and the JCM to investigate the nontrivial influence of CRW terms. Moreover, the AQRM possesses the same symmetry as the QRM, i.e., \mathbb{Z}_2 symmetry. Specifically, the eigenstate $|\phi_n\rangle$ of the system Hamiltonian $H_{\rm AQRM}$ satisfies $-\sigma_z e^{i\pi a^\dagger a} |\phi_n\rangle = \Pi |\phi_n\rangle$, with the parity eigenvalue $\Pi=\pm 1$. Hence, we are able to classify the eigenstates in the even and odd parity subspaces, which correspond to $\Pi=1$ and $\Pi=-1$, respectively.

B. Quantum dressed master equation

Practically, the hybrid quantum system inevitably interacts with the environment. To describe the influence of thermal baths on the AQRM, i.e., the qubit and the photon field individually coupled to two bosonic thermal baths, the total Hamiltonian is expressed as

$$H_{\text{total}} = H_{\text{AQRM}} + H_B + V,$$
 (2)

where the first term is just the AQRM Hamiltonian (1). Two bosonic thermal baths are described as $H_B = \sum_{u=q,c;k} \omega_k b_{u,k}^{\dagger} b_{u,k}$, where $b_{u,k}^{\dagger}$ ($b_{u,k}$) is the annihilation (creation) operator of bosons with the frequency ω_k in the uth bath. The interaction between the AQRM and two bosonic thermal baths is denoted as $V = V_q + V_c$, where two interaction terms associated with the qubit and the photon field read

$$V_q = \sum_k \lambda_{q,k} (b_{q,k} + b_{q,k}^{\dagger}) \sigma_x, \tag{3a}$$

$$V_c = \sum_k \lambda_{c,k} (b_{c,k} + b_{c,k}^{\dagger})(a+a^{\dagger}), \tag{3b}$$

with $\lambda_{q,k}$ ($\lambda_{c,k}$) the coupling strength between the qubit (photon field) and the corresponding bosonic thermal bath. Generally, the system-bath interaction can be characterized as the spectral function $\gamma_{q(c)}(\omega) = 2\pi \sum_k |\lambda_{q(c),k}|^2 \delta(\omega - \omega_k)$. In this work, we apply the Ohmic spectrum case to quantify the system-bath interaction [42], i.e., $\gamma_q(\omega) = \alpha_q \omega \exp(-\omega/\omega_c)/\Delta$ and $\gamma_c(\omega) = \alpha_c \omega \exp(-\omega/\omega_c)/\omega_0$, where $\alpha_{q(c)}$ is the systembath coupling strength, and ω_c is the cutoff frequency of bosonic thermal bath.

Under the assumption that the system-bath interaction is weak, we can separately perturb both V_c and V_q to obtain the DME by including Born-Markov approxi-

mation. Finally, the DME is described as [50, 53]

$$\frac{\partial \rho_{s}}{\partial t} = -i[H_{\text{AQRM}}, \rho_{s}]
+ \sum_{j,k>j} \{\Gamma_{u}^{j,k} [1 + n_{u} (\Delta_{k,j})] \mathcal{D}[|\phi_{j}\rangle\langle\phi_{k}|, \rho_{s}]
+ \Gamma_{u}^{j,k} n_{u} (\Delta_{k,j}) \mathcal{D}[|\phi_{k}\rangle\langle\phi_{j}|, \rho_{s}]\},$$
(4)

where the dissipator is $\mathcal{D}[O, \rho_s] = \frac{1}{2}(2O\rho_sO^{\dagger} - O^{\dagger}O\rho_s - \rho_sO^{\dagger}O)$, ρ_s is the reduced density matrix of the AQRM, $\Delta_{k,j} = E_k - E_j$ is the energy gap between two eigenstates (i.e, $|\phi_k\rangle$ and $|\phi_j\rangle$), $|n_u(\Delta_{k,j})| = 1/[\exp(\Delta_{k,j}/k_BT_u) - 1]$ is the Bose-Einstein distribution function, with k_B the Boltzmann constant and T_u the temperature of the u-th thermal bath, and the transition rates $\Gamma_q^{k,j}$ and $\Gamma_c^{k,j}$ are given by

$$\Gamma_q^{k,j} = \alpha_q \frac{\Delta_{k,j}}{\Delta} e^{-\frac{\Delta_{k,j}}{\omega_c}} |\langle \phi_j | (\sigma_- + \sigma_+) | \phi_k \rangle|^2,$$
 (5a)

$$\Gamma_c^{k,j} = \alpha_c \frac{\Delta_{k,j}}{\omega_0} e^{-\frac{\Delta_{k,j}}{\omega_c}} |\langle \phi_j | (a+a^{\dagger}) | \phi_k \rangle|^2.$$
 (5b)

Note that for only σ_{\pm} and linear photon operator appears in these expressions, the transitions are constraint between the eigenstates with different parities.

C. Two-photon correlation function

In quantum optics, the two-photon correlation function is widely considered as one powerful utility to measure the nonclassical radiation of photons, which also reflects the intrinsic correlation properties of quantum materials in light-matter interacting systems [1, 60–63]. The two-photon correlation function is defined as [48, 49]

$$G_2(\tau) = \frac{\langle a^{\dagger}(t)a^{\dagger}(t+\tau)a(t+\tau)a(t)\rangle}{\langle a^{\dagger}(t)a(t)\rangle^2},$$
 (6)

where $\langle \cdots \rangle$ stands for the mean value under the t-time reduced system density matrix. When the qubit-cavity coupling of the AQRM is sufficient weak, the output field is approximately proportion to the intracavity field. Thus, the photon statistic of the output field at the steady state can be properly described by Eq. (6). However, such definition may break down in the ultrastrong qubit-photon coupling regime [54].

To characterize the photon statistics at strong qubitphoton coupling, Ridolfo et al. [54–57] proposed a modified definition of the two-photon correlation function within the dressed picture, which overcomes the inconsistency that finite photon current occurs at the ground state. Consequently, the two-photon correlation function is re-defined as

$$G_2(\tau) = \frac{\langle X^-(t)X^-(t+\tau)X^+(t+\tau)X^+(t)\rangle}{\langle X^-(t)X^+(t)\rangle^2}, \quad (7)$$

where $\langle \mathcal{A} \rangle = \text{Tr}\{\rho_s(t)\mathcal{A}\}\$ stands for the mean value at the reduced density matrix $\rho_s(t)$, the detection operator X^+ in the dressed-state basis is expressed as

$$X^{+} = -i\Sigma_{j,k>j}\Delta_{kj}X_{j,k}|\phi_{j}\rangle\langle\phi_{k}|, \qquad (8)$$

with $X_{j,k} = \langle \phi_j | (a + a^{\dagger}) | \phi_k \rangle$ and $X^- = (X^+)^{\dagger}$. While for the representative zero-time delay case at the steady state, $G_2(\tau)$ is reduced to

$$G_2(0) = \frac{\langle X^- X^- X^+ X^+ \rangle_{ss}}{\langle X^- X^+ \rangle_{ss}^2},\tag{9}$$

where $\langle \cdots \rangle_{ss}$ denotes the expectation value at the steady state. As is well known, the bunching and antibunching features of photons are two representative non-classical phenomena of light [1, 49, 54]. The bunching behavior is characterized as $G_2(0) > 1$, which shows the super-Poisson distribution. $G_2(0) < 1$ denotes antibunching behavior of photons, corresponding to the sub-Poisson distribution. $G_2(0) = 2$ in the photon thermal field, whereas $G_2(0) = 1$ in the photon coherent state.

III. RESULTS AND DISCUSSIONS

A. Additional photon antibunching

We first investigate the influence of the anisotropic qubit-photon couplings on the two-photon correlation function $G_2(0)$ at the steady-state in terms of Eq. (9) at low temperature $(T_c = T_q = 0.07\omega_0)$. In Fig. 1 (a), we plot $G_2(0)$ as a function of g/ω_0 and r in a threedimensional view. To be more clear, we also present the contour of $G_2(0)$ with antibunching and bunching areas in Fig. 1 (b). The dissipative QRM result [55] is reproduced at r = 1. Intriguingly, multiple antibunchingto-bunching transitions of photons successively emerge with the increasing qubit-photon coupling in the highly anisotropic model, in sharp contrast to the isotropic case (r=1). In particular, the second antibunching signature is pronounced [e.g., $G_2(0)\approx 0.001$ at $g/\omega_0=1.6$ and r=0.4] and quite broad. This nontrivial feature has never been reported before. Hence, this provides an alternative routine to realize single-photon source based on deep strong anisotropic qubit-photon coupling systems [37]. When the anisotropic parameter approaches unity, the additional antibunching behavior is completely eliminated. This leaves only the single antibunching-bunching counterpart, similar to the dissipative QRM [55]. Therefore, we propose that the anisotropic coupling enriches the photon blockade effect in the dissipative qubit-photon interaction system.

Next, we derive an approximate expression of the twophoton correlation function at the steady state analytically. In the low temperature regime, the general relation of steady-state populations becomes $P_0 \gg P_1 \gg P_2 \gg P_3 \cdots$ $[P_n \propto \exp(E_n/k_B T)]$, under the assumption of finite energy-level spacing $\Delta_{kj} \gg k_B T$ $[\Delta_{kj} = (E_k - E_j)$, with

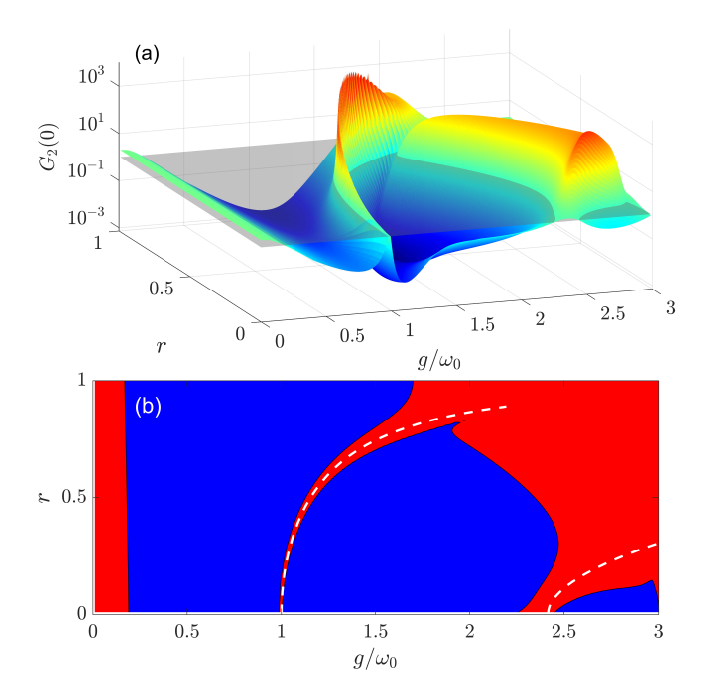


FIG. 1: (color online) (a) Three-dimensional view for the two-photon correlation function $G_2(0)$ of the dissipative AQRM at resonance $\omega_0 = \Delta$. For comparison we show the gray plane of $G_2(0) = 1$ to distinguish bunching and antibunching of photons. (b) Contour of $G_2(0)$ with antibunching and bunching marked in blue and red, respectively. The white dashed lines indicate the 1st-order QPTs of the closed AQRM. The other parameters are given by $\alpha_q = \alpha_c = 10^{-4}\omega_0$, $\omega_c = 10\omega_0$, and $T_q = T_c = 0.07\omega_0$.

 $E_k > E_j$ and $H_{\text{AQRM}} |\phi_k\rangle = E_k |\phi_k\rangle$]. For simplicity, the Hilbert space of AQRM is truncated to the subspace spanned by four lowest eigenstates of the AQRM, i.e., the ground state $|\phi_0\rangle$, and three low exited states $|\phi_1\rangle$, $|\phi_2\rangle$, and $|\phi_3\rangle$. Accordingly, the one-photon correlation term is estimated as $\langle X^-X^+\rangle_{ss} \approx \Delta_{1,0}^2 |X_{0,1}|^2 P_1$, which is contributed by the main transition $|\phi_0\rangle \rightarrow |\phi_1\rangle$. And the two-photon correlation term is given by $\langle X^-X^-X^+X^+\rangle_{ss} \approx \sum_{j < k < l, l \le 3} \Delta_{kj}^2 \Delta_{lk}^2 |X_{jk}X_{kl}|^2 P_l$, which is generally composed by four cooperative transitions, i.e., $|\phi_0\rangle \rightarrow |\phi_1\rangle \rightarrow |\phi_2\rangle$, $|\phi_0\rangle \rightarrow |\phi_1\rangle \rightarrow |\phi_3\rangle$, $|\phi_0\rangle \rightarrow |\phi_2\rangle \rightarrow |\phi_3\rangle$, and $|\phi_1\rangle \rightarrow |\phi_2\rangle \rightarrow |\phi_3\rangle$. Consequently, the two-photon correlation function is approximated as

$$G_{2}(0) \approx \frac{1}{\Delta_{1,0}^{4}|X_{0,1}|^{4}P_{1}^{2}} \times \left\{ \Delta_{1,0}^{2}|X_{0,1}|^{2}\Delta_{2,1}^{2}|X_{1,2}|^{2}P_{2} + \left[(\Delta_{2,0}^{2}|X_{0,2}|^{2} + \Delta_{2,1}^{2}|X_{1,2}|^{2})\Delta_{3,2}^{2}|X_{2,3}|^{2} + \Delta_{1,0}^{2}|X_{0,1}|^{2}\Delta_{3,1}^{2}|X_{1,3}|^{2}]P_{3} \right\},$$
(10)

which tightly relies on the transition coefficient X_{kj} between two eigenstates $|\phi_k\rangle$ and $|\phi_j\rangle$. Note that $X_{kj}=0$ if $|\phi_k\rangle$ and $|\phi_j\rangle$ are of the same parity, providing the selection rule of the correlation measurement induced eigenstate transition in the transition blockade $|\phi_k\rangle \rightarrow |\phi_j\rangle$.

In Fig. 2 (a), we plot the $G_2(0)$ curve for r=0.4.

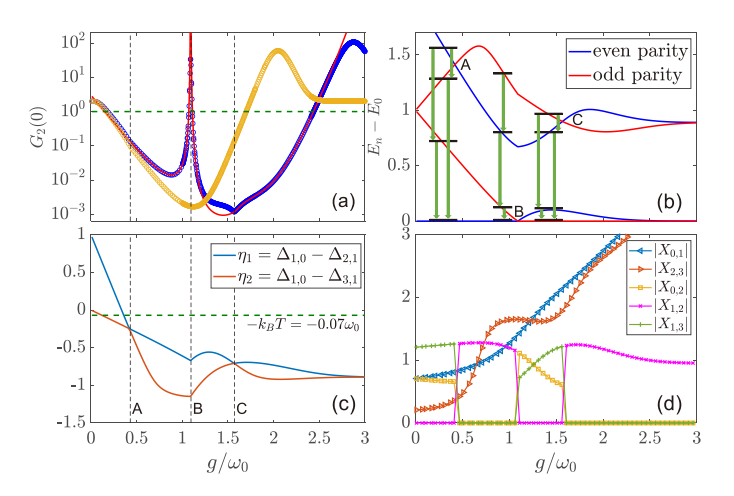


FIG. 2: (color online) (a) The comparison of $G_2(0)$ for the dissipative AQRM at r=0.4 between the numerical result and the corresponding analytical one from Eq. (10) denoted by blue circles and the red solid line, respectively. $G_2(0)$ for the dissipative QRM (r=1) is marked with yellow circles. (b) The energy spectra with different parities. A, B, C denote the corresponding energy level crossing points. The corresponding g's are also indicated with dashed lines in (a) and (c). The possible transitions between energy levels are denoted by green arrow lines. (c) η_1 in Eq. (12) and η_2 in Eq. (11). (d) The values of $|X_{jk}|$ with j < k. The other parameters are the same as in Fig. 1.

Interestingly, $G_2(0)$ in Eq. (10) is confirmed to agree well with the numerical result in a wide regime of the qubit-photon coupling. To understand the two photon correlation exhibited in Fig. 2 (a) based on the processes described in Eq. (10), we also present the relevant energy spectra $E_n - E_0$ in Fig. 2 (b). Then we proceed to analyze $G_2(0)$ in different coupling strength intervals below.

(i) In the regime $0.2 \lesssim g/\omega_0 \lesssim 0.45$, the measurement induced transition between $|\phi_1\rangle$ and $|\phi_2\rangle$ is prohibited $(X_{12}=0)$, due to the same odd parity of these two eigenstates denoted by red curves in Fig. 2 (b). Moreover, the upper transition $|\phi_2\rangle \rightarrow |\phi_3\rangle$ is inefficient compared to the process $|\phi_1\rangle \rightarrow |\phi_3\rangle$, because $|X_{23}| \ll |X_{13}|$. Hence, the two-photon correlation function can be further simplified as

$$G_2(0) \approx \frac{\Delta_{3,1}^2 |X_{1,3}|^2}{\Delta_{1,0}^2 |X_{0,1}|^2} \exp\left(\frac{\eta_2}{k_B T}\right),$$
 (11)

where $\eta_2 = \Delta_{1,0} - \Delta_{3,1}$ describes the anharmonicity of energy spectrum, shown by the brown solid line in Fig. 2 (c). It is found that the factor $\exp(\eta_2/k_BT)$ dominates $G_2(0)$. As the qubit-photon coupling strength increases, $\eta_2 < 0$ and decreases monotonically in this regime, so the factor $\exp(\eta_2/k_BT)$ is suppressed considerably at low temperatures. Thus, it is expected to observe such photon antibunching behavior, particularly in the regime $\eta_2 \ll -k_BT$.

(ii) In the regime $0.45 \lesssim g/\omega_0 \lesssim 1.05$, the suppressed transitions are quantified by $X_{02} = 0$ and $X_{13} = 0$, and

 $P_2\gg P_3$. Then, the two-photon correlation function can be approximately written as

$$G_2(0) \approx \frac{\Delta_{2,1}^2 |X_{1,2}|^2}{\Delta_{1,0}^2 |X_{0,1}|^2} \exp\left(\frac{\eta_1}{k_B T}\right),$$
 (12)

where $\eta_1 = \Delta_{1,0} - \Delta_{2,1}$. In this regime $G_2(0)$ is mainly characterized by the factor $\exp(\eta_1/k_BT)$ with the anharmonicity quantity η_1 displayed with the blue line in Fig. 2 (c). The persistent decay of η_1 thus leads to the pronounced photon antibunching behavior.

(iii) In the regime $1.15 \lesssim g/\omega_0 \lesssim 1.55$, the selection rule yields the transition blockade $|\phi_1\rangle \nrightarrow |\phi_2\rangle$ ($X_{12}=0$). Accordingly, we obtain the two-photon correlation function as

$$G_2(0) \approx \frac{1}{\Delta_{1,0}^4 |X_{0,1}|^4} \times (\Delta_{2,0}^2 |X_{0,2}|^2 \Delta_{3,2}^2 |X_{2,3}|^2 + \Delta_{1,0}^2 |X_{0,1}|^2 \Delta_{3,1}^2 |X_{1,3}|^2) \times \exp\left(\frac{\eta_2}{k_B T}\right) (13)$$

It is found that the nonlinear enhancement of Δ_{10} and reduction of Δ_{32} cooperatively contribute to the reentrance of the antibunching signal. As revealed in Fig. 2 (b) that the parity of the ground-state of AQRM at r = 0.4 can be reversed with the increasing coupling strength due to the level crossings of the first two eigenstates (c.f., Ref [11]). Entailed by the selection rule for the parities of the transition eigenstates, the dominant transitions are $|\phi_0\rangle \rightarrow |\phi_1\rangle \rightarrow |\phi_3\rangle$ and $|\phi_0\rangle \rightarrow |\phi_2\rangle \rightarrow |\phi_3\rangle$, which contributes to the pronounced photon antibunching with the valley behavior. This is distinct from the dominant transition processes in the QRM, i.e., $|\phi_0\rangle \rightarrow |\phi_1\rangle \rightarrow |\phi_2\rangle$, because the parity of the ground-state never changes with the coupling strength. Hence, the microscopic picture of the additional antibunching in the anisotropic QRM is different from the single antibunching in the isotropic case.

(iv) In the regime $1.5 \lesssim g/\omega_0 \lesssim 2.5$, the successive transition trajectories are the same as those in regime (ii) due to the selection rule for the parity of the lowest four energy levels, the two-photon correlation function in this regime is the same as Eq. (12).

Note from Eq. (10) that $G_2(0)$ diverges as $\Delta_{1,0}\rightarrow 0$. Combining with small contributions of other unimportant processes, the asymptotic trend of the energy level crossing between the ground state and the first-excited state lifts up the two-photon correlation function, resulting in a peak structure in the $G_2(0)$ curve around $g/\omega_0=1.1$. In the dissipative QRM, the energies of the ground state and the first-excited states never cross, and are only closer with the increasing coupling strength, thus the antibunching signal cannot reappear. The two detailed mechanisms proposed in (i) and (ii) actually also account for the traditional antibunching feature reported in the dissipative QRM, e.g., yellow circles in Fig. 2 (a).

Very interestingly, the third antibunching area emerges with further increasing the coupling strength for small anisotropic parameter r in Fig. 1 (b). In this regime, the processes discussed in the first antibunching area could

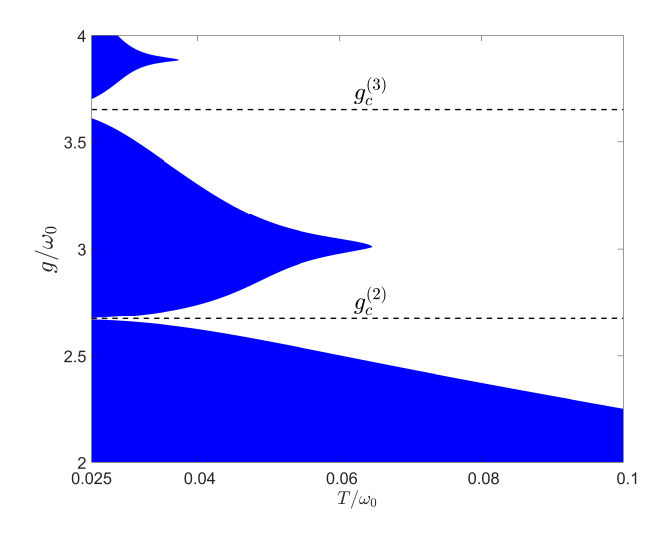


FIG. 3: (color online) The rescaled scheme of $G_2(0)$ with varying temperatures of thermal baths $T_q = T_c = T$ for AQRM at r = 0.2. Here photon antibunching (bunching) is denoted by the blue (white) color. The black dashed horizontal lines indicate $g_c^{(n)}$ of the 1st-order QPTs in the closed AQRM. The other system parameters are the same as in Fig. 1.

be applicable. Unlike the isotropic case, in the highly anisotropic model, Δ_{10} is enlarged again after the second level crossing of the first two eigenstates, which results in the antibunching feature again.

B. Implications of the photon bunching with the 1st-order quantum phase transitions

Xie et al. observed the first level crossing in the AQRM at $g_c^{(1)} = \sqrt{\frac{\omega_0 \Delta}{1-r^2}}$ using the Bargmann representation [36]. At the level crossing, the parity of the ground state changes sign and the system undergoes a 1st-order QPT. Within the Bogoliubov operator approach, Chen et al. [11] further revealed that the ground state and the first excited state can cross several times, indicating multiple 1st-order QPTs at $g_c^{(n)}$ with n a positive integer. Recently, Fink et al. experimentally characterized the 1st-order QPT by measuring two-photon correlation function in the driven-dissipative Bose-Hubbard system [64]. Then, it is interesting to see whether the 1st-order QPTs in the AQRM under the quantum dissipation can also be signified by the two-photon correlation function.

Specifically, there exists a significant photon-bunching peak in Fig. 1 (a) within the anisotropic parameter range $0 < r \lesssim 0.8$, which is also exhibited in detail in Fig. 2 (a) for r = 0.4. The behavior of the first critical point $g_c^{(1)}$ by tuning the anisotropic parameter r agrees well with the narrow photon-bunching regime, as indicated by the white dashed line in Fig. 1 (b). Furthermore, it is intriguing to find that the second critical coupling strength $g_c^{(2)}$ for the second 1st-order QPT derived in Ref

[11] can also be roughly captured by the photon-bunching feature with $r \lesssim 0.25$, as shown in Fig. 1(b).

To describe the implication of the two-photon correlation function with the 1st-order QPTs, we refine the detection signal of second 1st-order QPT by modulating two bath temperatures in Fig. 3. It is clearly shown that with the decreasing temperature, the photon bunching range monotonically shrink to the positions of the second and the third 1st-order QPTs denoted by the dashed lines.

Then, we analytically connect photon bunching feature with the 1st-order QPT of the AQRM. As the first excited state approaches the ground state, Δ_{10} vanishes gradually. In the low temperature regime, two-photon correlation function Eq. (10) is approximated as

$$G_2(0) \approx \frac{4(\Delta_{2,0}^2 |X_{0,2}|^2 + \Delta_{2,1}^2 |X_{1,2}|^2) \Delta_{3,2}^2 |X_{2,3}|^2 P_3}{\Delta_{1,0}^4 |X_{0,1}|^4},$$

with $P_1\approx 1/2$. As the qubit-photon coupling strength g approaches $g_c^{(n)}$, one-photon term $\langle \hat{X}^-\hat{X}^+\rangle \approx \Delta_{1,0}^2 |X_{0,1}|^2/2$ is strongly suppressed, which directly leads to the pronounced photon bunching feature.

Note from Ref. [11] that the numerical resolution of the level crossings is very difficult, especially in the deep strong-coupling regime, so it is challenging to identify the multiple 1st-order QPTs using the energy spectra. However, the signal of the two-photon correlation function, which is actually dependent on both the energy spectra and the eigenstates, is pronounced and quite obvious. Since the two-photon correlation function can be measured experimentally [61, 64, 65], we thus propose an alternative way to detect the locations of the 1st-order QPTs in this work.

Finally, we want to remark that the direct connection between the photon bunching feature and 1st-order QPTs in various QRMs is even popular, as long as the 1st-order QPT can occur. To demonstrate this point, we study the two-photon correlation function of the dissipative quantum Rabi-Stark model [66, 67] in Appendix. Since there is only a single 1st-order QPT in this model [68], we really find two antibunching area. The pronounced bouncing peak in between the two antibunching areas also signifies the 1st-order QPT. Therefore, we suggest that measuring photon bunching signal would generally characterize the 1st-order QPT of the qubit-photon hybrid systems.

IV. CONCLUSION

To summarize, we apply the quantum dressed master equation to investigate the nonclassical photon radiation in the dissipative AQRM, which enables us to properly treat the strong qubit-photon coupling. Then the two-photon correlation function at the steady state can be reasonably obtained, which generally shows more

than one successive antibunching-to-bunching transitions, in contrast to the traditional single antibunchingto-bunching transition in the isotropic QRM. In particular, the additional photon antibunching areas are explored in a wide parameter range of the strong qubitphoton interaction and finite anisotropic parameter, which is however unavailable in the QRM. We can also derive an approximate expression of the two-photon correlation function with lowest excitation populations in the low temperature regime, which quantitatively agrees well with the numerical results. The origin of such the additional photon antibunching effect is explained, based on the selection rule of the two-photon correlation measurement induced eigenstate transitions in the AQRM. Therefore, we provide an alternative platform to fertile the photon blockade effect and single photon source, via the anisotropic qubit-photon interaction.

Moreover, we study giant photon bunching effect at strong qubit-photon coupling. It is found that such photon bunching signal is highly related with the emergence of the 1st-order quantum phase transition, which is characterized as the level crossing of the ground state and first-excited state. Since the two-photon correlation can be measured experimentally, we hope that the analysis of photon antibunching and bunching effects in the anisotropic quantum Rabi model may deepen the understanding of nonclassical photon statistics in the qubitphoton hybrid systems, such as circuit quantum electrodynamics platforms. Finally, it should be noted that the present results are irrelevant with system-bath dissipation strengths, because weak interactions between the hybrid quantum system components, i.e., qubit and photons, and the corresponding thermal baths have been taken into account.

V. ACKNOWLEDGEMENTS

T. Y and Q.-H.C. are supported by the National Key Research and Development Program of China under Grant No. 2017YFA0303002 and the National Science Foundation of China under Grant No. 11834005. C.W. acknowledges the National Natural Science Foundation of China under Grant No. 11704093 and the Opening Project of Shanghai Key Laboratory of Special Artificial Microstructure Materials and Technology.

Appendix: Photon bunching in dissipative quantum Rabi-Stark model

The quantum Rabi-Stark model (QRSM) is formulated as [66, 67]

$$H_{\rm RS} = \omega_0 a^{\dagger} a + \frac{\Delta}{2} \sigma_z + U a^{\dagger} a \sigma_z + g \sigma_x (a + a^{\dagger}).$$
 (15)

By simulating the QRM with resonant Raman transition in ⁸⁷Rb atom interacting with high finesse cavity model

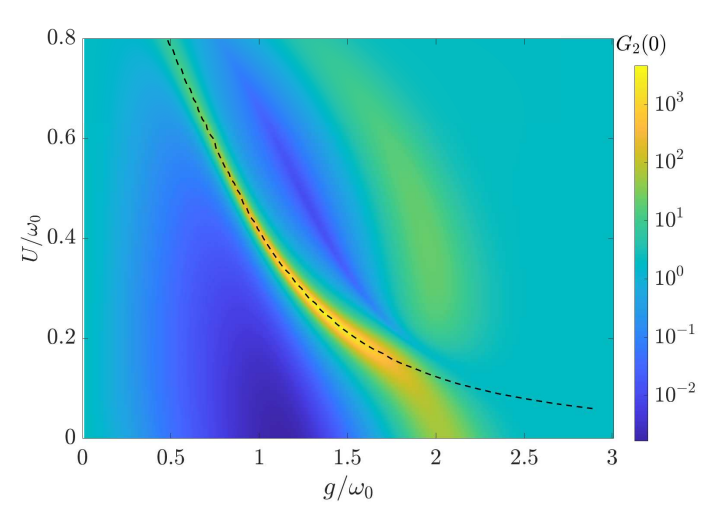


FIG. 4: (color online) The contour of $G_2(0)$ for the dissipative quantum Rabi-Stark model. The black dashed line denotes the 1st-order QPT of quantum Rabi-Stark model. The other system parameters are the same as in Fig. 1.

[66], a nonlinear coupling term $U\sigma_z a^{\dagger}a$ emerges, which is conceptually relevant to the dynamical Stark shift in quantum optics. There exist a single 1st-order QPT in the QRSM model when $|U/\omega_0| < 1$ [68].

We can also calculate the steady-state two-photon correlation function of the dissipative QRSM. As outlined in Sec. II B and II C for the dissipative AQRM, the steady state of the dissipative QRSM can be similarly solved by the quantum dressed master equation [50, 53]

$$\frac{\partial \tilde{\rho}_{s}}{\partial t} = -i[H_{RS}, \tilde{\rho}_{s}]
+ \sum_{j,k>j} \{\tilde{\Gamma}_{u}^{j,k} \left[1 + n_{u} \left(\tilde{\Delta}_{k,j} \right) \right] \mathcal{D}[|\tilde{\phi}_{j}\rangle\langle\tilde{\phi}_{k}|, \tilde{\rho}_{s}]
+ \tilde{\Gamma}_{u}^{j,k} n_{u} \left(\tilde{\Delta}_{k,j} \right) \mathcal{D}[|\tilde{\phi}_{k}\rangle\langle\tilde{\phi}_{j}|, \tilde{\rho}_{s}] \},$$
(16)

where the dissipator is $\mathcal{D}[O, \tilde{\rho}_s] = \frac{1}{2}(2O\tilde{\rho}_s O^{\dagger} - O^{\dagger}O\tilde{\rho}_s - \tilde{\rho}_s O^{\dagger}O)$ with $\tilde{\rho}_s$ the reduced density matrix of the dissi-

pative QRSM and $|\tilde{\phi}_{j(k)}\rangle$ the eigenstate of QRSM corresponding to eigenenergy $\tilde{E}_{j(k)}, H_{\rm RS}|\tilde{\phi}_{j(k)}\rangle = \tilde{E}_{j(k)}|\tilde{\phi}_{j(k)}\rangle$, $\tilde{\Delta}_{k,j} = \tilde{E}_k - \tilde{E}_j$ is the energy gap between the corresponding eigenstates, $n_u(\tilde{\Delta}_{k,j}) = 1/[\exp(\tilde{\Delta}_{k,j}/k_B\tilde{T}_u) - 1]$ is the Bose-Einstein distribution function, and the transition rates $\tilde{\Gamma}_q^{k,j}$ and $\tilde{\Gamma}_c^{k,j}$ are given by

$$\tilde{\Gamma}_{q}^{k,j} = \alpha_{q} \frac{\tilde{\Delta}_{k,j}}{\Delta} e^{-\frac{\tilde{\Delta}_{k,j}}{\omega_{c}}} |\langle \tilde{\phi}_{j} | (\sigma_{-} + \sigma_{+}) | \tilde{\phi}_{k} \rangle|^{2}, \qquad (17a)$$

$$\tilde{\Gamma}_{c}^{k,j} = \alpha_{c} \frac{\tilde{\Delta}_{k,j}}{\omega_{c}} e^{-\frac{\tilde{\Delta}_{k,j}}{\omega_{c}}} |\langle \tilde{\phi}_{j} | (a+a^{\dagger}) | \tilde{\phi}_{k} \rangle|^{2}.$$
 (17b)

Further, the steady-state two-photon correlation function $G_2(0)$ of dissipative QRSM is obtained by Eq. (9) with the detection operator X^+ reformulating as

$$X^{+} = -i\Sigma_{j,k>j}\tilde{\Delta}_{kj}X_{j,k}|\tilde{\phi}_{j}\rangle\langle\tilde{\phi}_{k}|,$$
 where $X_{j,k} = \langle\tilde{\phi}_{j}|(a+a^{\dagger})|\tilde{\phi}_{k}\rangle$ and $X^{-} = (X^{+})^{\dagger}$. (18)

The two-photon correlation function $G_2(0)$ of dissipative QRSM is displayed in Fig. 4, where the strong photon bunching regions are marked with yellow and chartreuse, whereas the strong photon antibunching regions are marked with the blue color. In the Stark coupling strength parameter range $0.2 \lesssim U/\omega_0 \lesssim 0.8$, there is a sharp bunching region which agrees with the transition points denoted by the black dashed line of the 1st-order QPT in QRSM $g_c^{\rm RS} = \sqrt{(\omega_0^2 - U^2)\Delta/(2U)}$ [68]. Interestingly, the bunching feature of photons characterizes the 1st-order QPT of QRSM in a wide parameter range.

For small Stark coupling $U/\omega_0 \lesssim 0.15$, the critical qubit-cavity coupling strength $g_c^{\rm RS}$ of the 1st-order QPT is quite big, the energy gap of the first two eigenstates after $g_c^{\rm RS}$ is too small to generate the antibunching feature, so the photon bunching cannot signify the 1st-order QPT. Owing to the same reason, in the nearly isotropic AQRM, as r is close to 1, the two-photon correlation function does not show a peak structure and cannot characterize the 1st-order QPT either, as shown in the Fig. 1(b).

M. O. Scully and M. S. Zubairy, Quantum Optics (Cambridge University Press, Cambridge, 1997); P. Meystre, Quantum Optics (Springer, Cham, 2021).

^[2] S. Haroche and J. M. Raimond, Exploring the Quantum: Atoms, Cavities, and Photons (Oxford University Press, Oxford, 2006).

^[3] M. Wallquist, K. Hammerer, P. Rabl, M. Lukin, and P. Zoller, Phys. Scr. T137, 014001 (2009).

^[4] G. Kurizki, P. Bertet, Y. Kubo, K. Mølmer, D. Petrosyan, P. Rabl, and J. Schmiedmayer, Proc. Natl. Acad. Sci. USA 112, 3866 (2015).

^[5] P. Forn-Díaz, L. Lamata, E. Rico, J. Kono, and E. Solano, Rev. Mod. Phys. 91, 025005 (2019).

^[6] A. F. Kockum, A. Miranowicz, S. De Liberato, S. Savasta, and F. Nori, Nat. Rev. Phys. 1, 19 (2019).

^[7] A. Blais, S. M. Girvin, and W. D. Oliver, Nat. Phys. 16, 247 (2020).

^[8] A. A. Clerk, K. W. Lehnert, P. Bertet, J. R. Petta, and Y. Nakamura, Nat. Phys. 16, 257 (2020).

^[9] M. J. Hwang, R. Puebla, and M. B. Plenio, Phys. Rev. Lett. 115, 180404 (2015).

^[10] M. X. Liu, S. Chesi, Z.-J. Ying, X. S. Chen, H.-G. Luo, and H.-Q. Lin, Phys. Rev. Lett. 119, 220601 (2017).

^[11] X. Y. Chen, L. W. Duan, D. Braak, and Q.-H. Chen, Phys. Rev. A 103, 043708 (2021).

^[12] Z. J. Ying, Adv. Quantum Technol. 4, 2100088 (2021).

- [13] M. L. Cai, Z. D. Liu, W. D. Zhao, Y. K. Wu, Q. X. Mei, Y. Jiang, L. He, X. Zhang, Z. C. Zhou, and L. M. Duan, Nat. Commun. 12, 1126 (2021).
- [14] A. Ronzani, B. Karimi, J. Senior, Y. C. Chang, J. T. Peltonen, C. D. Chen, and J. P. Pekola, Nat. Phys. 14, 991 (2018).
- [15] J. Senior, A. Gubaydullin, B. Karimi, J. T. Peltonen, J. Ankerhold, and J. P. Pekola, Commun. Phys. 3, 40 (2020).
- [16] J. P. Pekola and B. Karimi, Rev. Mod. Phys. 93, 041001 (2021).
- [17] C. Wang, H. Chen, and J. Q. Liao, Phys. Rev. A 104, 033701 (2021).
- [18] A. A. Anappara, S. De Liberato, A. Tredicucci, C. Ciuti, G. Biasiol, L. Sorba, and F. Beltram, Phys. Rev. B 79, 201303(R) (2009).
- [19] T. Niemczyk, F. Deppe, H. Huebl, E. P. Menzel, F. Hocke, M. J. Schwarz, J. J. Garcia-Ripoll, D. Zueco, T. Hümmer, E. Solano, A. Marx, and R. Gross, Nat. Phys. 6, 772 (2010).
- [20] F. Yoshihara, T. Fuse, S. Ashhab, K. Kakuyanagi, S. Saito, and K. Semba, Nat. Phys. 13, 44 (2017).
- [21] I. I. Rabi, Phys. Rev. 49, 324 (1936).
- [22] D. Braak, Phys. Rev. Lett. 107, 100401 (2011).
- [23] Q.-H. Chen, C. Wang, S. He, T. Liu, and K. L. Wang, Phys. Rev. A 86, 023822 (2012).
- [24] H. Zhong, Q. Xie, M. T. Batchelor, and C. Lee, J. Phys. A: Math. Theor. 46, 415302 (2013).
- [25] D. Braak, Q.-H. Chen, M. Batchelor, and E. Solano, J. Phys. A: Math. Theor. 49, 300301 (2016).
- [26] S. Haroche, M. Brune, and J. M. Raimond, Nat. Phys. 16, 243 (2020).
- [27] E. T. Jaynes and F. W. Cummings, Proc. IEEE 51, 89 (1963).
- [28] A. Baust, E. Hoffmann, M. Haeberlein, M. J. Schwarz, P. Eder, J. Goetz, F. Wulschner, E. Xie, L. Zhong, F. Quijandría, D. Zueco, J.-J. García Ripoll, L. Garca-Álvarez, G. Romero, E. Solano, K. G. Fedorov, E. P. Menzel, F. Deppe, A. Marx, and R. Gross, Phys. Rev. B 93, 214501 (2016).
- [29] A. Stockklauser, P. Scarlino, J. V. Koski, S. Gasparinetti, C. K. Andersen, C. Reichl, W. Wegscheider, T. Ihn, K. Ensslin, and A. Wallraff, Phys. Rev. X 7, 011030 (2017).
- [30] A. Bayer, M. Pozimski, S. Schambeck, D. Schuh, R. Huber, D. Bougeard, and C. Lange, Nano Lett. 17, 10, 6340 (2017).
- [31] J. Casanova, G. Romero, I. Lizuain, J. J. García-Ripoll, and E. Solano, Phys. Rev. Lett. 105, 263603 (2010).
- [32] Y.-Y. Zhang, Q.-H. Chen, S.-Y. Zhu, Chinese Physics Letters 30, 114203 (2013).
- [33] L. Garziano, V. Macrí, R. Stassi, O. Di Stefano, F. Nori, and S. Savasta, Phys. Rev. Lett. 117, 043601 (2016).
- [34] Z. Chen, Y. Wang, T. Li, L. Tian, Y. Qiu, K. Inomata, F. Yoshihara, S. Han, F. Nori, J. S. Tsai, and J. Q. You, Phys. Rev. A 96, 012325.
- [35] Y. X. Yu, J. Ye, and W. M. Liu, Sci. Rep. 3, 3476 (2013).
- [36] Q. T. Xie, S. Cui, J. P. Cao, L. Amico, and H. Fan, Phys. Rev. X 4, 021046 (2014).
- [37] A. Baksic and C. Ciuti, Phys. Rev. Lett. 112, 173601 (2014).
- [38] W.-J. Yang and X.-B. Wang, Phys. Rev. A 95, 043823 (2017).
- [39] G. C. Wang, R. Q. Xiao, H. Z. Shen, C. F. Sun, and K. Xue, Sci. Rep. 9, 4569 (2019).

- [40] S. I. Erlingsson, J. C. Egues and D. Loss, Phys. Rev. B 82, 155456 (2010).
- [41] I. C. Skogvoll, J. Lidal, J. Danon and A. Kamra, arXiv:2105.07430.
- [42] U. Weiss, Quantum Dissipative Dynamics (World Scientific, Singapore, 2012).
- [43] S. Schmidt, D. Gerace, A. A. Houck, G. Blatter, and H. E. Türeci, Phys. Rev. B 82, 100507(R) (2010).
- [44] M. J. Hwang, M. S. Kim, and M.-S. Choi, Phys. Rev. Lett. 116, 153601 (2016).
- [45] M. J. Hwang, P. Rabl, and M. B. Plenio, Phys. Rev. A 97, 013825 (2018).
- [46] H. J. Carmichael, Phys. Rev. X 5, 031028 (2015).
- [47] J. M. Fink, A. Dombi, A. Vukics, A. Wallraff, and P. Domokos, Phys. Rev. X 7, 011012 (2017).
- [48] H. J. Carmichael, Statistical Methods in Quantum Optics 1, Master Equations and Fokker Planck Equations (Springer, 1999).
- [49] R. J. Glauber, Phys. Rev. 130, 2529 (1963).
- [50] F. Beaudoin, J. M. Gambetta, and A. Blais, Phys. Rev. A 84, 043832 (2011).
- [51] A. Le Boité, M. J. Hwang, and M. B. Plenio, Phys. Rev. A 95 023829 (2017).
- [52] A. Settineri, V. Macrí, A. Ridolfo, O. Di Stefano, A. F. Kockum, F. Nori, and S. Savasta, Phys. Rev. A 98, 053834 (2018).
- [53] A. Le Boité, Adv. Quantum Technol. 3, 1900140 (2020);
 M.-S. Choi, *ibid.* 3, 2000085 (2020).
- [54] A. Ridolfo, M. Lieb, S. Savasta, and M. J. Hartmann Phys. Rev. Lett. 109 193602 (2012).
- [55] A. Ridolfo, S. Savasta, and M. J. Hartmann, Phys. Rev. Lett. 110, 163601 (2013).
- [56] A. Le Boité, M. J. Hwang, H. C. Nha, and M. B. Plenio, Phys. Rev. A 94, 033827 (2016).
- [57] L. Garziano, A. Ridolfo, S. De Liberato, and S. Savasta, ACS Photonics 4, 2345 (2017).
- [58] M. Radulaski, K. A. Fischer, K. G. Lagoudakis, J. Y. Linda Zhang, and J. Vučković, Phys. Rev. A 96, 011801(R) (2017).
- [59] J. B. Curtis, I. Boettcher, J. T. Young, M. F. Maghrebi, H. Carmichael, A. V. Gorshkov, and M. Foss-Feig, Phys. Rev. Research 3, 023062 (2021).
- [60] Q. Schaeverbeke, R. Avriller, T. Frederiksen, and F. Pistolesi, Phys. Rev. Lett. 123, 246601 (2019).
- [61] S. H. Cantu, A. V. Venkatramani, W. C. Xu, L. Zhou, B. Jelenković, M. D. Lukin, and V. Vuletić, Nat. Phys. 16, 921 (2020).
- [62] A. S. Prasad, J. Hinney, S. Mahmoodian, K. Hammerer, S. Rind, P. Schneeweiss, A. S. Sørensen, J. Volz, and A. Rauschenbeutel, Nat. Photon. 14, 719 (2020).
- [63] Q. Bin, X.-Y. Lü, F. P. Laussy, F. Nori, and Y. Wu, Phys. Rev. Lett. 124, 053601 (2020).
- [64] T. Fink, A. Schade, S. Höfling, C. Schneider, and A. Imamoglu, Nat. Phys. 14, 365 (2018).
- [65] D. E. Chang, V. Vuletić, and M. D. Lukin, Nat. Photon. 8, 685 (2014).
- [66] A. L. Grimsmo and S. Parkins, Phys. Rev. A 87 033814 (2013).
- [67] H.-P. Eckle and H. Johannesson, J. Phys. A: Math. Theor. 50, 294004 (2017).
- [68] Y. F. Xie, L. W. Duan, and Q.-H. Chen, J. Phys. A: Math. Theor. 52, 245304 (2019).